Printed Passive Microfluidic Devices using TEOS Reactive Inks

by

Yiwen Huang

A Thesis Presented in Partial Fulfillment
of the Requirements for the Degree
Master of Science

Approved April 2016 by the
Graduate Supervisory Committee:

Owen Hildreth, Chair
Robert Wang
Konrad Rykaczewski

ARIZONA STATE UNIVERSITY

May 2016

ABSTRACT

This paper details ink chemistries and processes to fabricate passive microfluidic devices using drop-on-demand printing of tetraethyl-orthosilicate (TEOS) inks. Parameters space investigation of the relationship between printed morphology and ink chemistries and printing parameters was conducted to demonstrate that morphology can be controlled by adjusting solvents selection, TEOS concentration, substrate temperature, and hydrolysis time. Optical microscope and scanning electron microscope images were gathered to observe printed morphology and optical videos were taken to quantify the impact of morphology on fluid flow rates. The microscopy images show that by controlling the hydrolysis time of TEOS, dilution solvents and the printing temperature, dense or fracture structure can be obtained. Fracture structures are used as passive fluidic device due to strong capillary action in cracks. At last, flow rate of passive fluidic devices with different thickness printed at different temperatures are measured and compared. The result shows the flow rate increases with the increase of device width and thickness. By controlling the morphology and dimensions of printed structure, passive microfluidic devices with designed flow rate and low fluorescence background are able to be printed.

ACKNOWLEDGEMENTS

TABLE OF CONTENTS

LIST OF TABLES

LIST OF FIGURES

Chapter 1. INTRODUCTION

Passive fluidic devices are widely used in the disease diagnosis and pathogen detection [1] [2]. A successful forms of such diagnostic tests is the lateral flow assay (LFA), which typically uses a paper based membrane [3]. A common device that has experienced great success is the pregnancy test strip for the detection of human chorionic gonadotropin (hCG). A typical LFA requires a membrane that provides a solid support for receptor adsorption and fluid transport among other desirable properties and functions. However the typical LFA has some major setbacks. It is desirable to have sensitive detection systems for the early detection of diseases and LFAs do not meet this requirement. Also, since the test is mostly colorimetric it requires visual inspection/interpretation by the user, thus most LFA tests are only qualitative at best. There is a demand for low cost, disposable, reliable, sensitive, and robust test devices, especially for poor resource areas. Our approach attempts to address the issue of sensitivity using fluorescence detection, rather than colorimetry. Fluorescence is a result of light-matter interactions where a material absorbs light, causing electronic state excitation and a subsequent re-emission of light at a lower frequency (higher wavelength/Stoke shift). [4] Fluorescent dyes could be attached to nanoparticles or more specifically, directly use as a label attached to an antibody. One can then take advantage of the highly specific antigen-antibody interactions for biomarker detection.

A typical fluorescence setup comprises a light source (Halogen, Mecury, Laser, LED, etc), optical filters (excitation and emission filters), and a detector (CMOS, CCD, PMT, photodiode, etc). The emission filter is used to create a narrow band source from a wide

spectrum source, which is then used to excite the fluorophores attached to the sample. The fluorophores when excited at a specific wavelength, emit light at a longer wavelength. This emitted light is filtered using the emission filter, which also serves to block the excitation light from reaching the detector, so that only the fluorophore emission is detected by the detector. Non-idealities in filters and detector assembly, as well as background in the substrate/membrane used in the system, lead to light reaching the detector, thus decreasing the signal-to-noise ratio (SNR). Most polymeric membranes do exhibit some level of background fluorescence, especially paper based membranes and animal tissue. The high background evident in paper based membranes e.g. nitrocellulose, which is the gold standard for most LFA, limits the sensitivity of fluorescence based LFA. It is therefore important to be able to develop a membrane that has the desirable properties of nitrocellulose, but also has a low background, which doesn't limit the sensitivity of fluorescence based LFA. Such a material must have pore sizes that range from 8 to 15 μm, a strong affinity for proteins, and be stable and suitable for low cost manufacturing.

TEOS (tetraethyl-orthosilicate) are widely used in spin coating and chemical vapor deposition to make thin silica films. [5] As silica is chemically stable and transparent, it is potentially a very good material to be used as a solid support for fluorescent LFA due to its porosity and relatively low background compared to paper, shown in Figure1. For most of the application of TEOS, it is used after it is fully hydrolyzed. The chemical hydrolysis reaction in TEOS solution generates many nano particles dispersed in the solution. Particle size analysis are usually 8nm [6]. The hydrolysis reaction happens continuously once the solution is made.

2

In this paper, 3D inkjet printing is investigated as a new method of TEOS fabrication. A 3D structure like paper helps increase sensitivity and improve the lower limit of detection by increasing the surface-area-to-volume ratio when compared to 2D membranes like glass slides. In order to have the ability of printing 3D porous structures with any designed patterns and thickness, people usually use fully hydrolyzed TEOS ink. In this paper, structures, or microfluidic devices printed by ink having almost no hydrolysis time (reactive ink) are also discussed. By visual and SEM inspection, structures printed using fully hydrolyzed ink show highly fracture morphology. However, structures printed by reactive ink show much more solid morphology. Liquid can flow through fracture structure due to the capillary action of liquid along cracks inside the devices. Most importantly, this printed fracture structure shows almost no background in the green light excitation test.
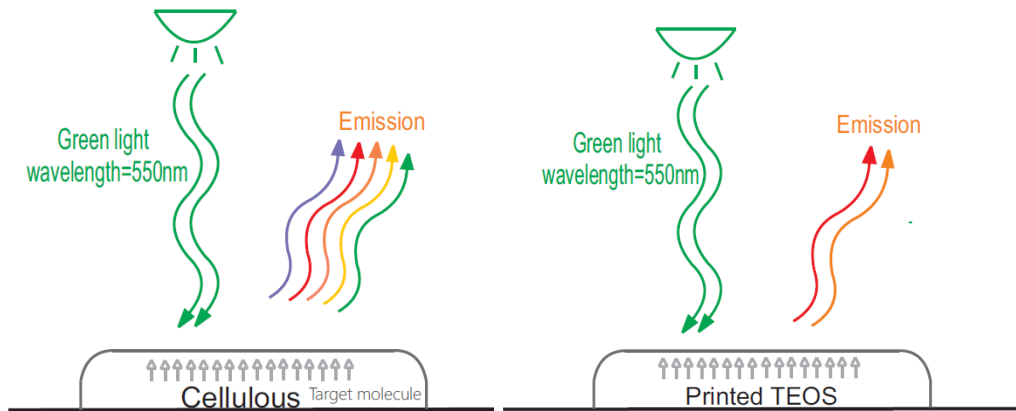
Figure 1. Fluorescence performance of cellulous and printed TEOS when shined by green light

Chapter 2. EXPERIMENTAL METHODS

2.1 TEOS sol-gel preparation

2.1.1 Preparation of the SiO$_2$ Sol

Before adapting it to the specific requirements of inkjet printing, a polymeric SiO$_2$ sol was prepared following a standard procedure published by Uhlhorn and by de Lange.[7][8] In preliminary tests, a commercial spin-on-glass (NDG-1000 Undoped glass, DS04092014, Desert Silicon, Inc) product is used to verify the printing possibility. But in further experiments, we made our own sol for printing. Synthesis of this sol began with the solution of the precursor tetraethyl-orthosilicate (TEOS, C8H20O4Si; Alfa Aesar, headquartered in Ward Hill, Massachusetts) at room temperature. Then, controlled hydrolysis of the precursor was achieved by adding a mixture of ethanol, water and hydrochloric acid. After complete addition of the acidic mixture, the ratio of the components was TEOS/Ethanol/H$_2$O/HCl = 0.0941/0.3597/0.5722/0.008 (mol%) = 0.4/0.4/0.194/0.006(volume%). Two types of sol were made for inkjet printing, one was called reactive ink, which means the sol was diluted and printed immediately after the acidic mixture is added. However, during the process of printing, loading the ink and printer alignment takes several minutes, so strictly speaking, the reactive ink have 5-10 minutes hydrolysis time. The other type of ink is fully hydrolyzed ink, which was stirred constantly during hydrolysis. The obtained sol was kept at 60 ℃ in a water bath for 3 h to complete hydrolysis and condensation reactions, resulting in weakly branched polymeric SiO$_2$ structures. Both stock sol had a transparent appearance. Particle size analysis

revealed a size of ~8 nm [6]. All inks subsequently used for inkjet printing were prepared from the same stock sol.

2.1.2 *Modification of the SiO₂ Sol for Inkjet Printing*

In the case of many inkjet printing processes, the most important properties of the ink are viscosity and boiling point of solvents used. In our printing process, SiO_2 stock sol is usually further diluted adding ethanol, methanol and 1-propanol. These dilutions are required to keep the proper requirements (viscosity) for inkjet printing. In preliminary tests, it was found that spin-on-glass dilution with ethanol was able to inkjet print and form very porous structure since the diluted sol has proper viscosity. However, ethanol's boiling point is 78℃, therefore the printing temperature is required to be low, and so the ethanol won't be a proper choice of diluents. So, we chose methanol (boiling point 64℃) as an alternative diluent. For the same reason, we chose 1-propanol as an alternative diluent for high temperature printing. 1-propanol is an alcohol that is easily miscible with the SiO_2 sol, but with reduced vapor pressure and slightly increased viscosity compared to ethanol [η (1-propanol) = 1.938 mPa s; η (ethanol) = 1.074 mPa s, both at ambient temperature]. It is therefore more suitable for the operating viscosity range of the Spectra printer head used. Dilution of the SiO_2 stock sol with 1-propanol by a ratio of 1/5 was found to be optimal to ensure stable processing conditions during inkjet printing. The diluted sol was filtered before being filled into the ink container by using a 25mm Syringe filter with a 0.45μm Nylon membrane (VWR international, North American Cat No.28145-489) to clean the inks of dust and particle agglomerations.

2.2 Inkjet printer and print head

A commercial inkjet printer (Jetlab II Precision Printing Platform [10]) was used in this study (Figure. 2). This high precision printing platform was suited for laboratory usage to evaluate and develop inkjet materials, processes and applications. The Jetlab II printer consists of a motion system, a substrate table with a dimension of 200 to 200 mm, an electronic pressure control and alignment system to determine the exact position of the substrates, a printhead assembly, and a drop view system which allows to analyze the volume and the speed of the drops of each nozzle from the printhead in real time. The precise motion platform allows an overall accuracy of 5 μm of the printed structures and consists of X, Y and Z axis for the movement of the printhead assembly and the substrate table.

Figure 2. Jetlab 2 pricision priting platform

The printhead assembly was equipped with the ink supply system, an electronic pressure control and a custom printer head. This custom printhead is designed based on a DIY printhead from the internet. [9] We designed 5 versions of printheads (Figure.3). In fig. 4, this is a schematic image of the printhead, the function of the nozzle was based on the action of piezoelectric element [10]. All these elements are covered and compressed by 3D printed Nylon structures. When piezoelectric element was applied as a pulse, it moved horizontally. When the element moved to the left, it generated a vacuum inhaling the ink from supply tube; when the element moves to the right, it squeezed the liquid out from the bottom nozzle and then form micro droplets, shown in Figure 4. The nozzle used here is actually micro pipette pulled from a capillary tubes.   By adjusting the pulse wave form and applying back pressure, the drop size, velocity, diameter and velocity can be controlled. With the improvement of each version, their printing performance has a significant change. This printhead is a low cost product; the total cost is about than 10 dollars. One of its significant advantage is it can be easily repaired especially the nozzle. During the printing, the micro size nozzle can be clogged very easily, so, it requires the nozzle to be replaceable. With our custom printhead, a clogged nozzle can be easily replaced by a new nozzle in 10 minutes. This does not only save the money but save a lot of time to unclog commercial nozzles. To avoid continuous ink flow through the nozzles, the ink container was evacuated. Optionally, the printer head can be heated up to 150 ℃, which makes it possible to research how the printing behaves at high temperatures. For the latest version, we can assemble any nozzle with diameter from 30 micros to 150 micros. Correspondingly, the size of droplets can vary from 10pL to 1000pL, the drop

velocity varies from 0.5m/s to 6m/s and the diameter of droplets varies from 10 micros to 130 micros.
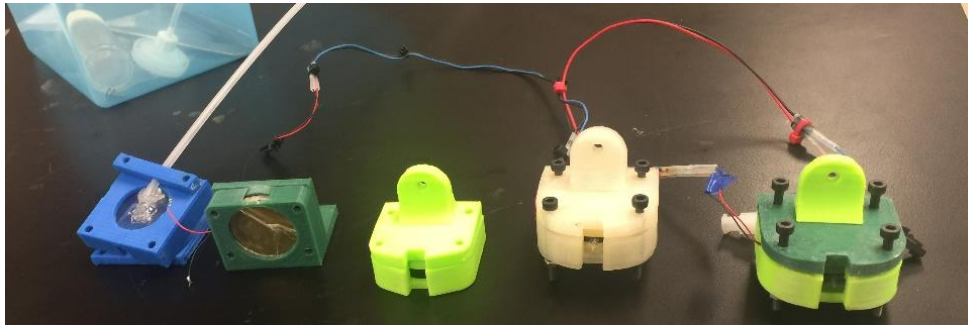
Figure 3. Iteration of custom printhead, from left to right are version 1, 2, 3, 4, 5 respectively, right second one is for high temperature (150℃) printing and the right-most one is for normal temperature printing (Room temperature to 100℃)
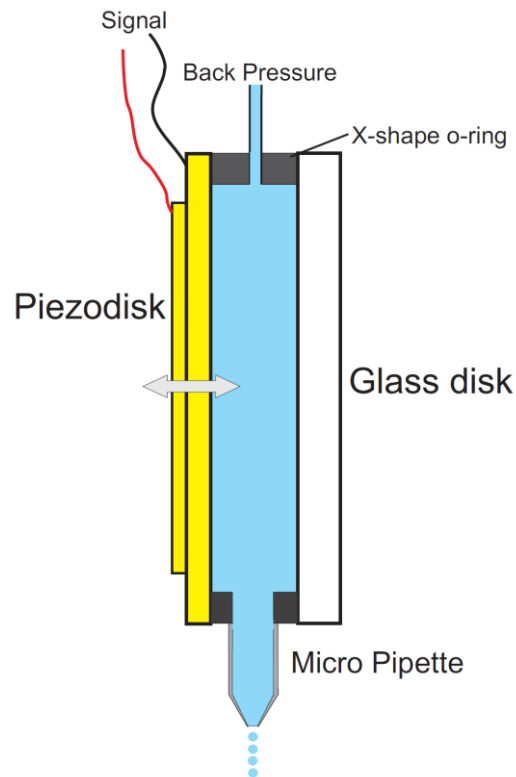
Figure 4. Cross section schematic of piezoelectric disk driven printhead. Piezoelectric disk is driven by square wave signal and move horizontally, causes the volume change of inner chamber and then generate micro droplets.

2.3 Printing and metrology

Signal							Vacuum	Frequency
Rise time1	Dwell time	Fall time	Echo time	Rise time2	Idle time	Voltage		
20μs	200μs	20μs	200μs	20μs	0μs	±55V	-0.1 psi	200 Hz

Table 1. Standard operation and printing parameters used for TEOS printing in this paper.

Our custom printhead was driven by the signal generated by Jetlab II Precision Printing Platform. The ink container is vacuumed by a precision pressure control system. Table. 1 shows the standard operation parameters and printing parameters consistently used in this work. Usually, the piezoelectric element in the printhead was working under a ±55V square wave input signal whose dwell time and echo time are both 200 μs. But under some special cases such as bad nozzle quality, in order to keep the consistence of printing quality, the voltage may vary from 45V to 55V and the dwell time and echo time can also vary from 120μs to 300μs. The vacuum value of ink container was adjusted depends on the size of nozzle assembled. Typically, the smaller nozzle we use, the higher vacuum were used. However, there still is a range of vacuum value (-0.01 psi to -0.2 psi) according to the range of nozzle's inner diameter, usually from 30 μm to 100μm. As substrate can be heated from room temperature up to 200℃, our custom printhead can usually functionally keep working from room temperature up to 150℃. The humidity of printing environment keeps 20% constantly.

Two series of samples were printed for each experiments, one group of TEOS ink was printed directed on a cleaned silicon wafer for morphology observation and profilometry measurement while the other was printed on a thin film of polyimide (McMASTER-

9

CARR, part number, 2271K1) on glass slides. Because polyimide will prevent the wicking and spread of low viscosity liquid, so the fluid flow tested on the polyimide substrate can represent the reasonable true fluid flow speed. Though the silicon wafer used were directly taken from original packages, the whole process was not operated in clean room. So, there may be a chance that dust particles could fall down on the substrate during the printing process even the printing environment were always kept clean. For both series of samples printed, the same script file were loaded, which programmed the printer to print a line which is actually 200×1 array with dots spacing of 70 micros. In order to make sure there is about 10-15% area overlap between adjacent dots the diameter of droplets was controlled to be 30 micros usually with 12pL to 18pL volume, shown in Figure 5. We consider one printing cycle of the array a single layer, samples with multiple layers, usually 1, 5, 10, 20, 30, 40, 50 layers, were printed. Fluid flow rate were measured for samples printed with different layers on polyimide. The thickness of SiO_2 layers in dependence on the number of layers were measured by profilometer (The Dektak XT™ stylus profiler, Bruker Corporation) and some cross section image from SEM (Array 1990).
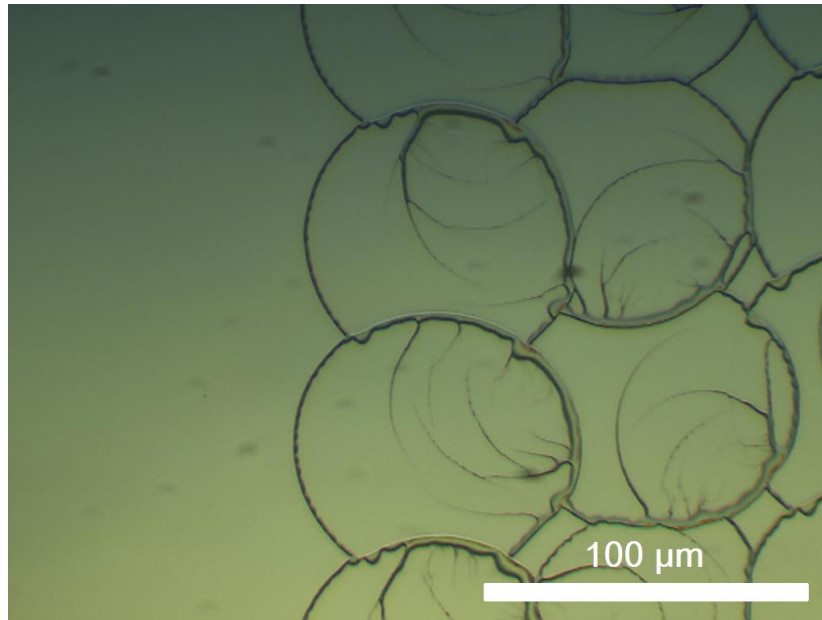
Figure 5. Optical image of printed single layer array with 70μm dots spacing and dots' diameter 80μm. Approximate 10-15% overlap between dots are observed.

2.4 Flow rate measurement

The principle of passive fluidic device is basically the capillary action of liquid. Capillary action (sometimes capillarity, capillary motion, or wicking) is the ability of a liquid to flow in narrow spaces without the assistance of, or even in opposition to, external forces like gravity [11]. It occurs when the adhesion force between liquid face and solid surface is bigger than the resistance force such as gravity and pressure.

To measure the fluid flow speed, we use the simplest and the most direct definition. Figure 12 shows the method of measurement. We dripped a micro droplet of ethanol solution (1:1 with water) dyed blue whose volume is 1μL using a precision pipette. Then the ethanol solution wicked along the printed TEOS lines until it did not move any further. The whole measurement process was recorded by a Dinoscope (Dino-Lite Premier2 Digital Microscope, AD4113TL-R4), the distance fluid flows were measured

11

from the interface between droplet and line to the point where fluid stops. Also, the time was counted from the according video recorded. Thus, the result of dividing the distance by time is the average flow speed (mm/s) of fluid. However, due to the slightly width difference of each print lines due to substrate temperatures, printed layers, and instability of equipment. Therefore, we introduce a new data: flow speed per unit width (1/s) which is the result of dividing average flow speed by the width of the line. By normalizing flow speed by this way, the flow speed are comparable for all printed samples.

Fluid flow data of samples printed at 50, 75, 100, 125, 150℃ are measured. For each temperature, 7 samples are printed with different printing layers which are 1, 5, 10, 20, 30, 40, 50 layers. Totally flow speed of 35 samples were measured and for each sample both flow speed and flow speed per unit width are shown in the result.

2.5 *Fluorescence Background Measurement*

As we discussed in previous words, fluorescence performance is one of crucial characteristics of printed microfluidic devices. So, we took some printed samples and use a fluorescence reader to measure the light intensity of the background fluorescence.
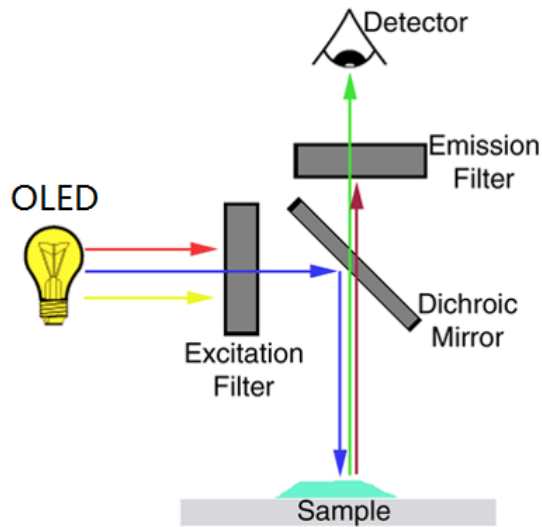
Figure 6. Working principle of fluorescence microscopy used to measure the background fluorescence of samples

Figure 6 shows the working principle of a lab build fluorescence microscopy. Our reader have the same working principle with it. First of all, the whole test procedures were completed in a dark room. An OLED light shines from the bottom and the then filtered by a green light filter assembled above the OLED light. When the green light comes from the filter, it was shined on the sample directly from bottom and generated fluorescence emission due to the material's property. Then the fluorescence emission went through an emission filter and was detected by a photodiode detector above the emission filter. The signal from photodiode detector were amplified and then transfer to digital data.

Those data measured was mainly shown as the voltage-time chart and normalized background intensity values. A temperature dependence of background (auto-fluorescence) signal in passive fluidic device printed at 6 temperatures is finished at clean room. Therefore, the fluorescence from other contaminates can be excluded from the

13

result. All the TEOS precursors and solvents were consistently used for every test. Samples are printed with precursors diluted by methanol, ethanol and 1-propanol (volume ratio 1:5) respectively. For each type of ink, samples are printed on glass slides at room temperature (22℃), 50, 100, 150, 200, and 300 ℃. High temperature such as 200 and 300 ℃ are extension experiments for future test, but there result are also discussed in this paper. 18 samples were made totally.

Chapter 3. RESULTS AND DISCUSSION

Morphology and structure play very crucial role in passive fluidic devices' performance. We found three printing parameters could affect the printed morphology and inner structure. First, printing temperature have a great impact of evaporate rate of solvents, therefore printed morphology are affected. In addition, in order to print fracture structures at relative low temperature (<75℃), methanol was introduced as one of the solvents, other two are ethanol and 1-propanol. Most importantly, the time of TEOS's hydrolysis reaction dramatically changed the printed morphology. Two types of ink were made, one is reactive ink with 0 minutes hydrolysis time, the other one is fully hydrolyzed ink with 180 minutes hydrolysis time. Different morphology were observed from samples printed using inks diluted by different solvents at different temperatures. Morphology are observed by scanning electron microscope and thickness are mainly measured by profilometer. Three impacts of morphology are shown and discussed below.

3.1 Morphology vs. Temperature

As introduced in the printing process, we focused on three parameters which could affect printed morphology, which are t_H= hydrolysis time before loading ink, T_s= substrate temperature = 50, 75, 100, 125, 150℃ and three diluting solvents: methanol ($T_{boiling}$=64℃), ethanol ($T_{boiling}$=78℃) and 1-propanol ($T_{boiling}$=64℃). In this section, we mainly focus on the impact of substrate temperature though hydrolysis time and solvents also affect the morphology. From SEM images of all printed samples, we observed substrate temperature mainly changes the morphology by the difference of evaporate rate

of solvent at different temperatures. Though the boiling point of methanol, ethanol and 1-propanol have obvious difference, their evaporate rate all increase with the increase of substrate temperature. For a specific volume of droplets, its drying time can be calculated.

Figure 8 shows the SEM morphology of 12 samples printed on silicon wafer with reactive ink (t_H=0min) diluted by methanol, ethanol and 1-propanol at substrate temperature from 50℃ to 125℃. The room humility was 20% and temperature is 27.7℃. From drop inspection system, we got the parameters of droplets generated. For a single droplet, its average velocity is 5.46m/s with volume 16.6pl and diameter 31.67μm. As introduced before, one printing layer is actually 1 by 200 array with dots spacing 70μm. So the length of printed device is approximate 14mm. All the samples in Figure 8 have 50 printing layers.

In Figure 8, from left to right, morphology printed at different temperatures are compared. It looks like two lines are printed on substrate in 50℃'s images no matter which solvents are used for dilution. However, there was only one line printed at the right middle of the image. The reason for this phenomenon is called coffee ring effect [12]. The surfactant-mediated interactions between particles and the liquid−gas (LG) and liquid−solid (LS) interfaces, rather than the flow patterns, primarily define the morphology of the dry deposit in a robust and reproducible manner. For like-charged particle/surfactant mixtures, most of the particles form a ring-shaped deposit, but some particles can also be deposited inside the ring in a way that is modulated by electrostatic interactions between the particles and the LS interface. In addition, from profilometry data, coffee ring effect are verified by thickness of cross section. Although it looks there is no difference between substrate and the middle area of lines, thickness of middle area

16

is about 6μm while the thickness for 1 layer sample is about 100nm. For the thickness of edge (ring area), the thickness is about 14μm while for 1 layer is about 600nm. Also, due to the low substrate temperature, droplet spread a lot after it land on substrate. So the width of the lines are much wide than the droplets' diameter.
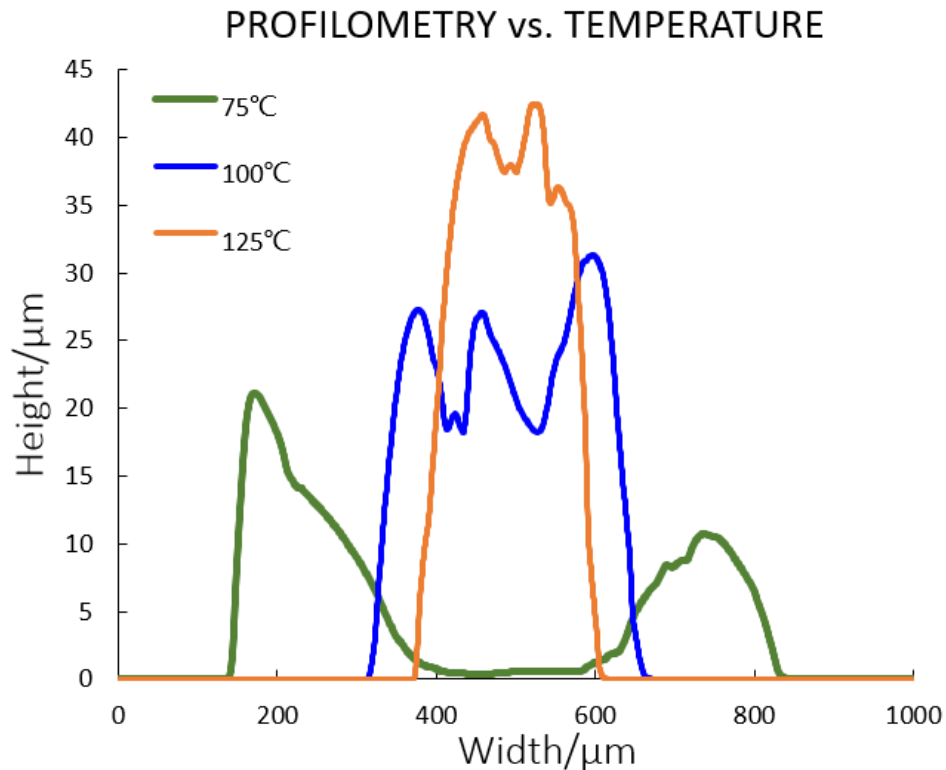
PROFILOMETRY vs. TEMPERATURE

Figure 7. Profilometry data of 50 layers samples printed with reactive ink diluted by 1-propanol at 75, 100, 125℃

As substrate temperature increases, evaporate rate of solvent also increases. After a droplets landed on the substrate, due to the rapid evaporation of solvent, it does not spread as much as at low temperature. In addition, due to the increase of evaporation rate, coffee ring effect was not observed as obviously as samples printed at low temperatures. Most importantly, the width decreases with the increase of substrate temperature. Figure

7 shows the profilometry data of samples printed with 1-propanol diluted reactive ink at 75, 100 and 125℃. The width of sample printed at 75℃ is about 700 microns while for sample printed at 125℃, the width decreases to 200 microns. Because these three samples are printed at the same condition, their volume are basically the same. Bacause of the same amount of materials were printed, as width decreases, the height should increase. As observed in Figure 7, the height of printed samples changes from 20 μm to 40 μm with substrate temperature increases from 75℃ to 125℃. This means we can achieve higher printing precision and control the width of the device by changing substrate temperature. The decrease of width can be obviously observed from the result using methanol and 1-propanol diluted inks. But for samples using ethanol diluted ink, this phenomenon is not obvious. The width of the thinnest line observed among all samples in Figure 7 is 200 microns. In addition, in Figure 7, the cross section shape of sample printed at 125℃ is trapezoidal, this is because fluid flow, surface tension, viscosity and evaporate rate of ink when it is printed layer by layer.

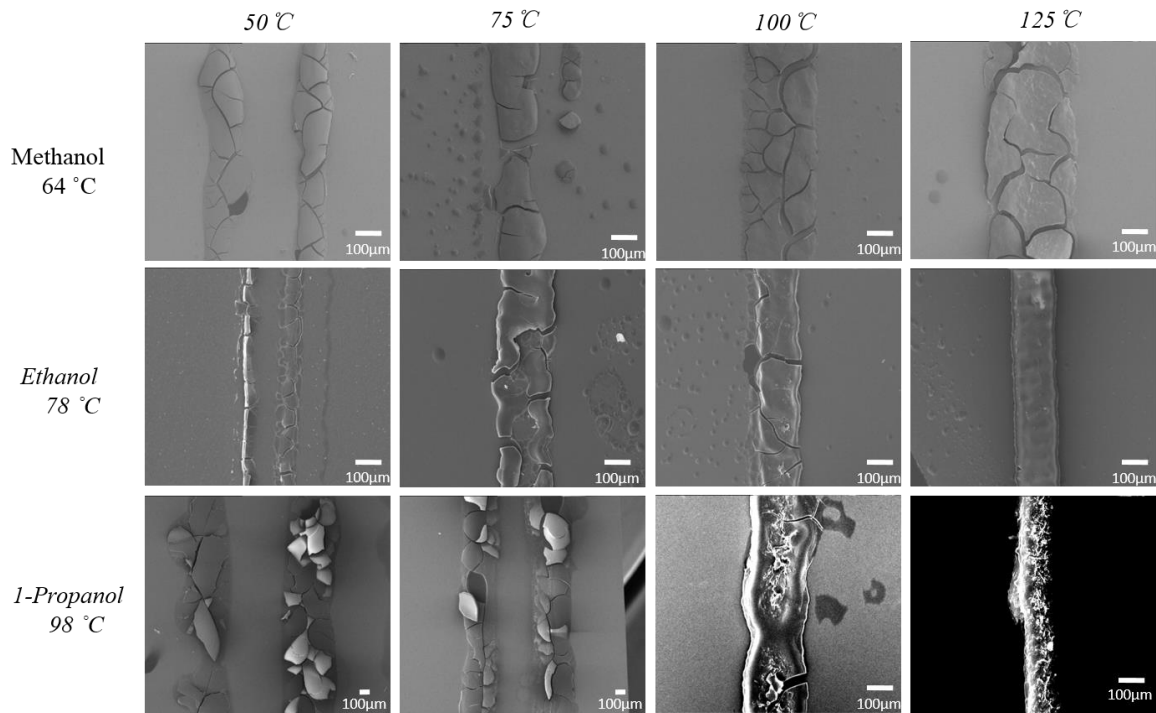|	50 ℃	75 ℃	100 ℃	125 ℃
Methanol 64 ℃				
Ethanol 78 ℃				
1-Propanol 98 ℃				

Figure 8. Top view SEM images of samples printed using methanol, ethanol and 1-propanol at different temperatures. The width of lines decreases with the increasing of temperature.

In Figure 8, more cracks are observed on the surface of samples printed at low temperatures than high temperatures. For sample printed using ethanol diluted ink at 125℃, we observed the most dense surface and inner structure. We think the main reason samples show more cracks at low temperature is its low evaporate rate. Once the solvents stay on the substrate, it actually provides a time for TEOS's hydrolysis. When TEOS is fully hydrolyzed, nano-particles are dispersed in the solution. After solvents are dried out, the cracks happen between the weak points between nanoparticles. However, at higher temperatures, due to the rapid evaporate of solvents, there is no enough time for TEOS to be fully hydrolyzed and dry. Which means the hydrolysis reaction happens at the same time of solvents' evaporation. Thus, chemical bonds are generated and are usually stronger than the bond force between particles. This explains why the cracks are more

19

easily happened and the size of single structure piece is smaller at lower temperatures. Fracture structures also indicates the evaporate rate at droplets' surface is usually higher than the inside. Thus, SiO_2 firstly solidified at the part close to the surface which forms the shield morphology observed at lower temperatures in Figure 8.

3.2 *Morphology vs. solvents*

In other inkjet printing method, such as dip coating and spin coating process, in order to keep the costing thickness or thin film's thickness, TEOS sol-gel is usually diluted by adding ethanol and 1-propanol [7]. Our experiments follows their dilution method and we found the best concentration for dilution is TEOS sol-gel: solvents = 1:5. This dilution ratio make sure the droplets were stable and the printed passive fluidic devices were working properly. Structures printed at high temperature can be very fracture by using hydrolyzed ink and it's because the rapid evaporation rate of solvents at high temperature. However, from fluorescence test result, it's found that the background increases slightly with the increase of printing temperature. In order to keep the same fracture morphology but lower the printing temperature, a solvent who has the similar liquid properties with organic solvents like ethanol and 1-propanol but with lower boiling point is needed. Methanol meets these requirements and then it is used as one of the solvents used for dilution. Thus, printed structure using inks diluted by methanol, ethanol and 1-propanol are comparable.

Six samples are printed for comparison, reactive and fully hydrolyzed TEOS sol-gel are diluted by methanol, ethanol and 1-propanol with volume ratio 1:5 respectively. All the samples are printed at100℃ for 50 layers. Room humility is 20%.

20

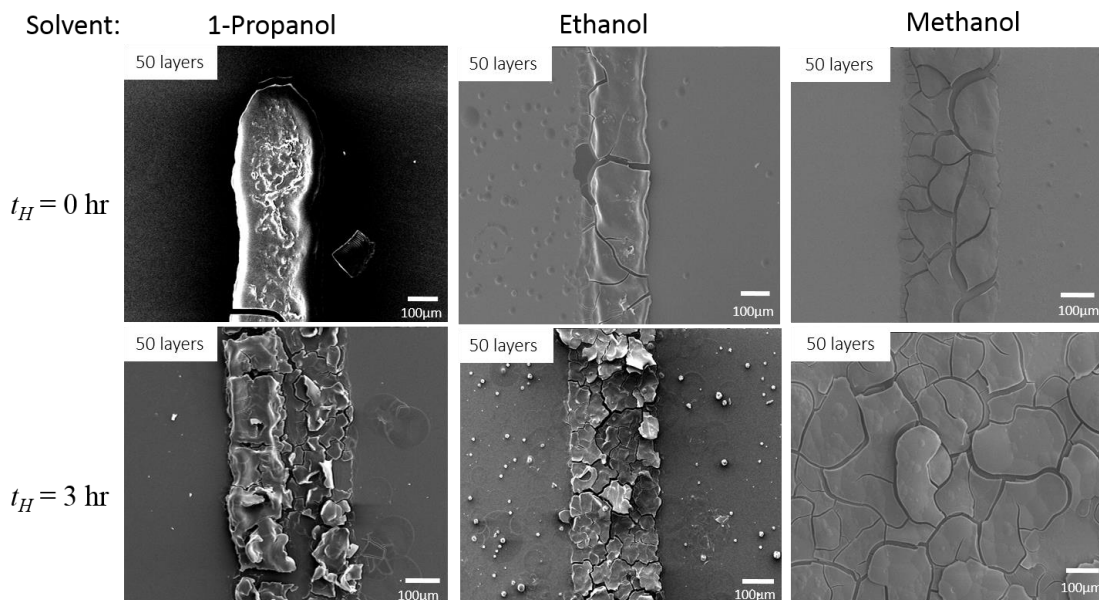| Solvent:	1-Propanol	Ethanol	Methanol

$t_H = 0$ hr

$t_H = 3$ hr

Figure 9. Morphology of printed line using reactive and fully hydrolyzed inks diluted by methanol, ethanol and 1-propanol. More cracks are shown in lines printed using methanol than the one using 1-propanol and ethanol.

Figure 9 shows the top view SEM images of six samples. Each column are using the inks diluted by same solvent and each row represent the same hydrolysis time. By comparison of the first row's result, it is observed samples using methanol diluted ink show more cracks than using ethanol diluted ink while samples printed using ethanol diluted ink shows more cracks than using 1-propanol diluted ink. The width of lines basically keep the same. The difference of surface morphology is due to the difference of solvents' property. One of the key properties is their boiling point. The boiling point of methanol, ethanol and 1-propanol are 64, 78 and 98 ℃ respectively. As samples are printed at 100℃, solvents like methanol and ethanol whose boiling point is far low than 100℃ are evaporated rapidly after they reached the substrate. Due to their fast evaporation rate, those solvents require more space and generate bigger fluid flow force. This may explain the different size and number of cracks between samples

21

diluted by different solvents. Ethanol has higher boiling point than methanol, thus it shows less and smaller cracks on the surface. We assume for ink diluted by 1-propanol, the evaporation rate is the most reasonable among all three inks, which gives the result that most of the parts are solid without cracks. Also, a slightly increased molecule size of 1-propanol compared to ethanol (kinetic molecule diameter d (1-propanol) = 0.47 nm; d (ethanol) = 0.43 nm) was assumed to influence the nanostructure of the SiO_2 layer only marginally. [7]

However, by using fully hydrolyzed TEOS sol-gel, difference between solvents were not as obvious as reactive ink. As shown in Figure 9 second row, all three samples show many cracks on the surface and have fracture structure. The difference between solvents did not affect the morphology when using fully hydrolyzed ink. One possible explanation is hydrolysis time of TEOS sol plays the most crucial role instead of dilution solvents. Details are shown and discussed in next section.

3.3 Morphology vs. Hydrolysis time

As discussed in the previous sections, solvents and substrate temperature can affect the morphology. However, most importantly, hydrolysis reaction can dramatically affect the printed morphology. By changing the hydrolysis time of TEOS sol-gel, morphology can vary from very solid to very fracture. In this section, results from reactive (no hydrolysis time) and fully hydrolyzed inks are discussed. Two types of ink are made, they are all diluted by ethanol with 1:5 volume ratio and printed by the same nozzle at 125℃. The only difference is the hydrolysis time before the ink was loaded. Figure 10 shows the top

view and cross section with three magnification of printed lines. The top surface of sample is very flat and no cracks are observed. In cross section view, the sample was put up side down because the sample pilled off from silicon wafer and moved the position in the sample box. In order to protect the sample, we didn't turn it over. So the top surface is facing down in the cross section image. It is observed that the height of this sample is about 15μm and cracks or pores are barely found at cross section and top surface. It shows it has a very dense structure and high quality. In higher magnification cross section images, uneven and discontinuous surface are observed. We assume the inner structure is actually a multilayers dense solid. The interface between layers is not even, but in each layer, the structure is solid. The formation of those layers depends on the printing process. 50 layers were split to 10 times printing, so per five layers were printed continuously. Droplets were inspected per five layers and it takes about 20 seconds. This short time gap between per five layers causes the layers structure.
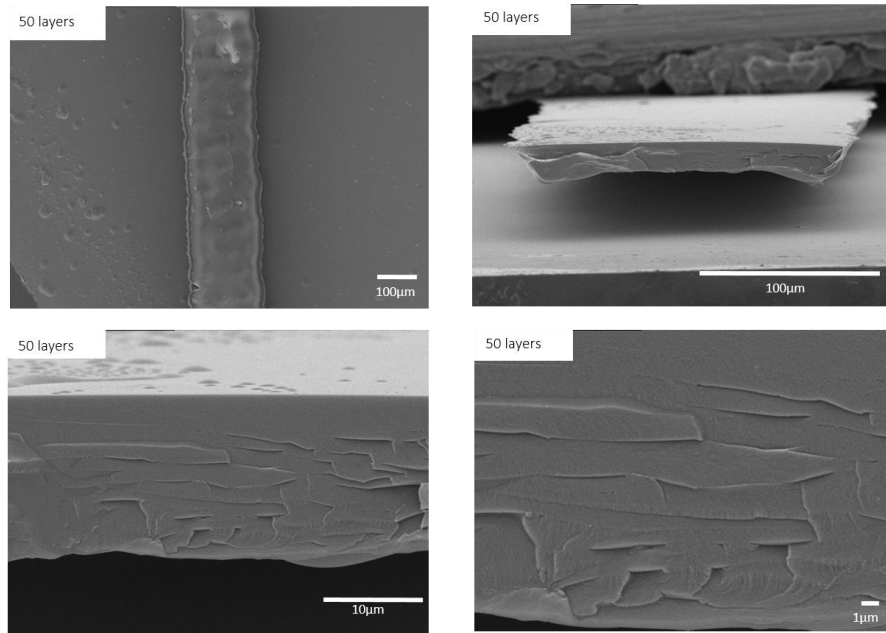
Figure 10. Top view and cross section view of printed lines using ethanol diluted reactive ink at 125℃. Solid layer by layer structures are observed in high magnification images.

Figure 11 shows the morphology of samples printed with fully hydrolyzed ink. From those images, very fracture structure and rough surface are observed. From higher magnification images, different size cracks are observed. The biggest crack width is about 10 microns while small cracks are usually 1 micron wide. This morphology is an ideal one to be passive microfluidic device. Those cracks are like capillaries and fluid flows along cracks due to capillary action.
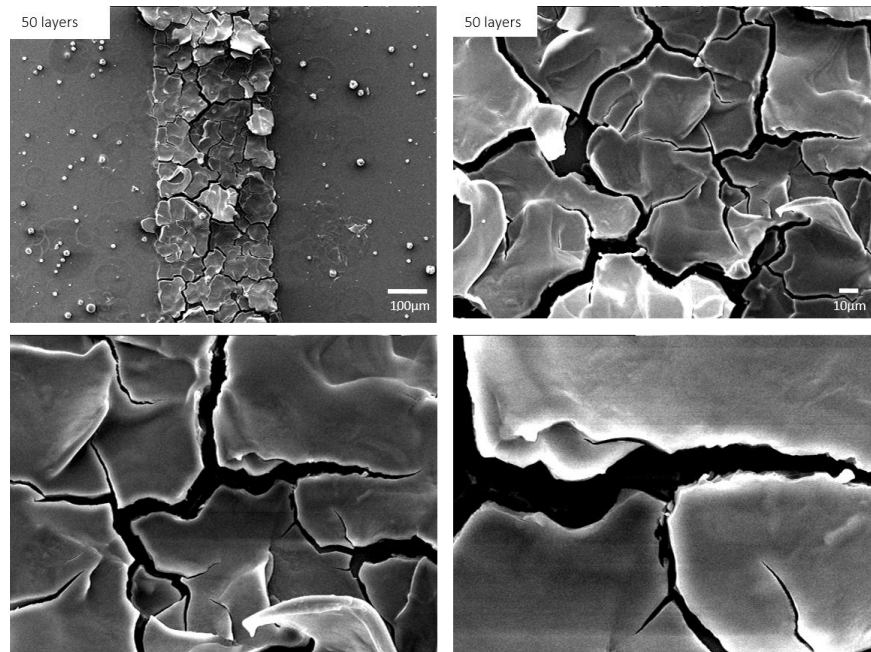
Figure 11. Top view of printed lines using ethanol diluted fully hydrolyzed ink at 125℃, fracture morphology and rough surface form ideal condition for capillary action.

The morphology's difference coms from their different printing regime. For reactive inks, the hydrolysis of TEOS in solution happens mainly on the substrate in a very short time. Droplets usually have an overlap between each other, so this makes the line are

formed continuously with the TEOS's hydrolysis reaction. SiO_2 molecules are tightly arranged and form the dense inner structures. However, thing are totally different for fully hydrolyzed ink. During 3 hours hydrolysis, huge amount of nano SiO_2 particles are produce and dispersed in the solution [13]. Some nano particles may come together and form larger particles. So, fully hydrolyzed ink is like particles inks, after solvents are evaporated out, those particles left and forms porous material. The bond force between each particles or groups are much weaker than the bond force between molecules. Thus, the impact from solvents evaporation and fluid flow can easily brake those physical bonds and form cracks. As mentioned before, those cracks are the key of passive microfluidic devices.

3.4 Flow rate

A passive fluidic device is mainly used to transport liquid. So flow rate is a very important property for it. As we found samples with fracture structure and rough surface are the ideal devices. We printed 7 samples with different layers (1, 5, 10, 20, 30, 40, 50 layers) at 5 temperatures (50, 75, 100, 125, 150℃). Figure 12 shows the method of measurement. The first step is dripping a micro droplets (1μL) of ethanol solution (1:1 volume with water) dyed blue from a pipette onto one end of printed lines. Then the fluid will flow along the line and eventually stops wicking. All the process was recorded and time *t* fluid flows are obtained from the video. In addition, the length *l* and width *d* are measured by microscope.
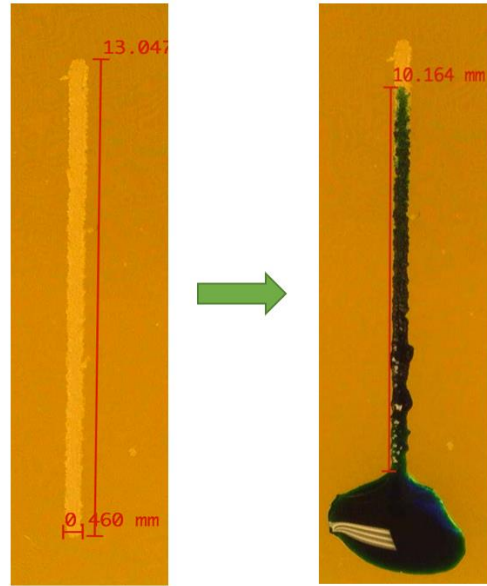
Figure 12. Flow rate measurement method of printed passive microfluidic devices

The flow speed V is calculated by dividing l by t. However, printing temperature causes the difference of line width. It is observed that fluid flows faster in wider lines because wider lines have less resistance force. So, we divide V by the width of the line and get v which is called flow speed per unit width. Thus, interference factor from width is cancelled.

Figure 13 shows the flow speed and flow speed per unit width for each sample printed. Results for samples printed at 50℃ are not shown because no valid results are obtained. In figure 13, the same trend was observed that V & v increases with the thickness's increasing. For samples printed at 50℃ the first valid data is collected by the 30 layers samples and for samples printed at 75℃, the first valid data was collected from 20 layers. Both 5 layers samples printed at 125℃ and 150℃ gave valid Flow speed data.
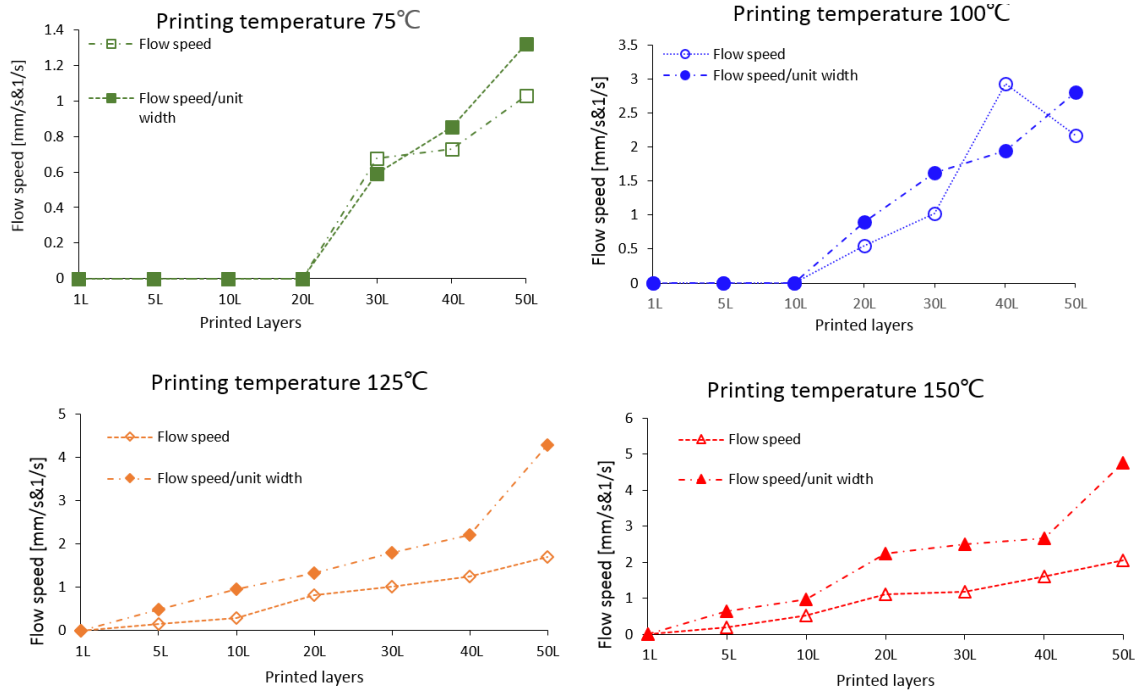
Figure 13. Flow speed and flow speed per unit width *vs.* printed layers at 75, 100, 125, 150℃

In figure 14, flow speed per unit width *v* at different temperatures are compared. As shown in the chart, flow speed per unit width is higher when printing temperatures are higher. This is because higher temperature usually gives highly fracture structure while low temperature doesn't.
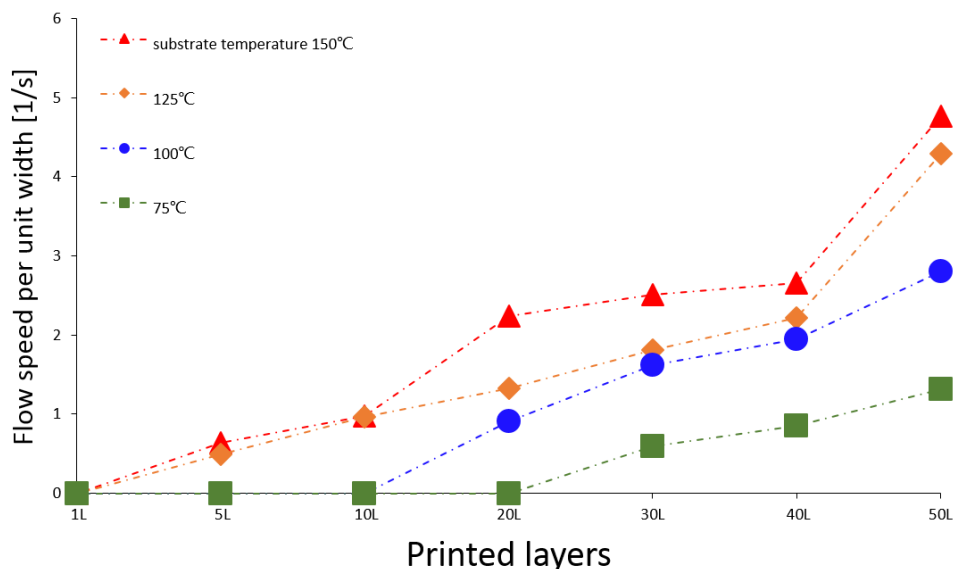
27

Figure 14. Comparison of flow speed per unit width *vs.* printed layers at different substrate temperatures

3.5 *Fluorescence background test*

A temperature independence of background (auto-fluorescence) signal in printed SiO_2 was designed and done by a fluorescence reader. Inks were diluted by methanol, ethanol and 1-propanol and then printed substrate at room temperature, 50, 100, 150, 200, 300℃. Higher temperature like 200 and 300℃ were designed for future work. Figure 15, 16, 17 show all the results measured. In histogram, black dash line represents the background intensity of 10pg/mL Dylight550 which is the lowest value used in previous work. Red dash line represents the back ground of glass slides. In Figure 15, background intensity increases with the increase of substrate temperature, the same trend are also observed in Figure 16 and 17. We are still searching the reason.

28
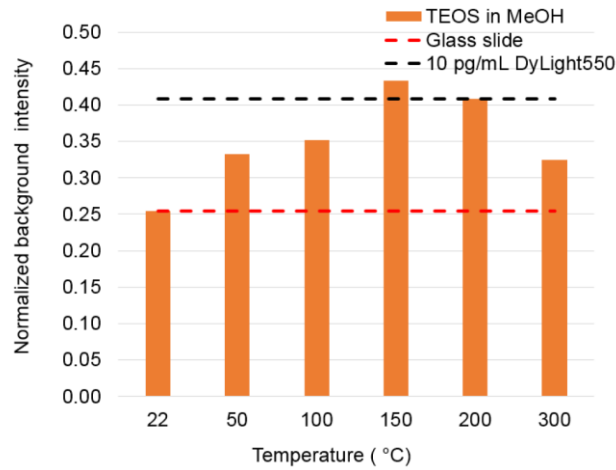
Figure 15. Normalized background intensity comparison between TEOS in methanol, glass slide and 10pg/mL Dylight550.

However, the results shows the background intensity of samples printed using methanol diluted ink at most substrate temperatures are below the lowest value we made before. Background intensity of sample printed at 150℃ is slightly higher than the lowest value.
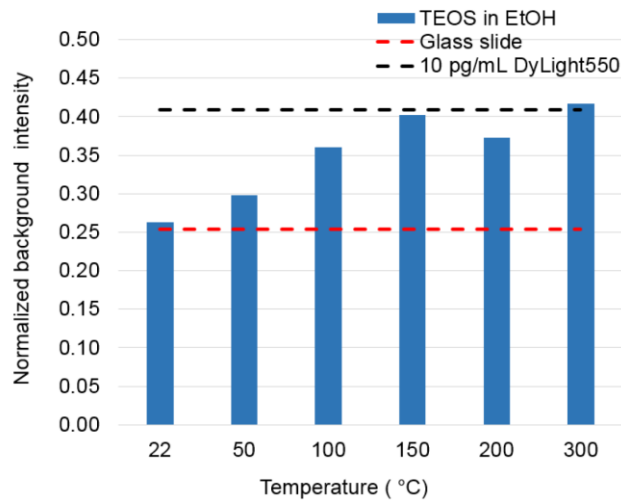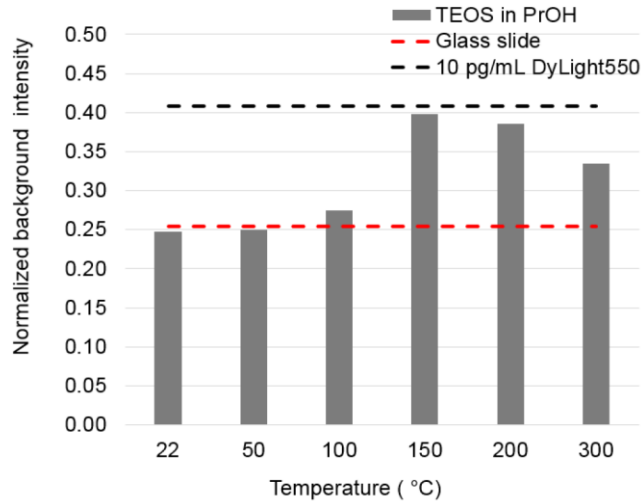

Figure 16. Normalized background intensity comparison between TEOS in ethanol, glass slide and 10pg/mL Dylight550.

Figure 17. Normalized background intensity comparison between TEOS in

1-propanol, glass slide and 10pg/mL Dylight550.

In Figure 16 and 17, background intensity of all samples are below the lowest value. By comparing all the results, it is found at room temperature, all the inks show no background, but the highest background of all inks happens at 150℃. It is surprisingly found that TEOS diluted by 1-propanol printed at 100℃ almost show no background when compared with glass slide. Thus, also considering about the impact of temperature to morphology, it's better to print passive microfluidic devices using 1-propanol diluted ink at 100℃ substrate temperature.

Chapter 4. CONCLUSION

In summary, passive microfluidic devices can be successfully made by 3D inkjet printing. All the experiments are completed by a custom inkjet printhead assembled to a commercial 3D inkjet printer. Standard TEOS sol-gels are made and then diluted by methanol, ethanol, and 1-propanol (with volume ratio solvents:TEOS = 5:1) to meet the requirement of inkjet printing and fracture structure. Two types of TEOS sol-gel were made based on the hydrolysis time of TEOS. One is reactive ink (no hydrolysis time), the other is fully hydrolyzed ink. From SEM images of printed samples, the hydrolysis time of TEOS plays a dramatic role in morphology. Very dense structures are observed by printing ethanol diluted reactive ink at 125℃, while very fracture structure and rough surface are observed by using fully hydrolyzed ink printed at the same temperature. Substrate temperatures also affect the printed morphology. First, width of lines decreases if printed at higher temperature. Second, structure is more fracture and the surface is rougher if printed at a higher substrate temperature. This happens because solvents' evaporation rate is faster at higher temperatures and it reduced the width of droplets' spread on substrate. Also, faster evaporation rates require more space and generates stronger inner fluid flow which will cause the cracks to occur. Printed samples show different morphology using inks diluted by different solvents due to the difference of their boiling point. The boiling point of methanol, ethanol, and 1-propanol are 64, 78, and 98℃ respectively. They show different evaporation rate when printed at the same substrate temperature which causes the difference of morphology. Flow speed is the main characteristic for a passive microfluidic device. We measured the flow speed and flow

31

speed per unit width for samples printed at different temperatures and layers. The result shows that no matter the flow speed or flow speed per unit width, they all have the same trend, which is they increase with the increase of printed layers. By comparing the flow speed *vs*. temperature, it is found higher temperatures give higher flow speed. The range of flow speed per unit width varies from 0 to 5 *1/s.* In addition, fluorescence background test shows all the samples are below the lowest value and approximately 50% of the samples have the similar value as glass slide. This means we are able to print passive microfluidic devices with reasonable flow rate and low fluorescence background.

REFERENCES

[1] Kirby, B.J. (2010). Micro- and Nanoscale Fluid Mechanics: Transport in Microfluidic Devices. Cambridge University Press.

[2] Karniadakis, G.M., Beskok, A., Aluru, N. (2005). Microflows and Nanoflows. Springer Verlag

[3] Wong, Raphael, Tse, Harley (Eds.) Lateral Flow Immunoassay ISBN 978-1-59745-240-3

[4] M. Sauer, J. Hofkens, and J. Enderlein Handbook of Fluorescence Spectroscopy and Imaging. 2011 WILEY-VCH Verlag GmbH & Co. KGaA, Weinheim ISBN: 978-3-527-31669-4

[5] Kenneth R. Spring & Michael W. Davidson, Introduction to Fluorescence Microscopy,
http://www.microscopyu.com/articles/fluorescence/fluorescenceintro.html

[6] Bulla, D.A.P; Morimoto, N.I (1998). "Deposition of thick TEOS PECVD silicon oxide layers for integrated optical waveguide applications". Thin Solid Films 334: 60. doi:10.1016/S0040-6090(98)01117-1.

[7] Martin Bram, Jurgen GmbH Inkjet printing of microporous silica gas Separation Members, J.Am. Ceram. Soc 98 [8] 2388-2394(2015)

[8] R. S. A. de Lange, J. H. A. Hekkink, K. Keizer, and A. J. Burggraf, "Permeation and Separation Studies on Microporous Sol–Gel Modified Ceramic Membranes," Microporous Mater., 4, 169–86 (1995).

[9] Adrian Bowyer, An inkjet head that can be completely made in a RepRap machine, http://reprap.org/wiki/Reprappable-inkjet

[10] MicroFab an ink-jet innovation company TECHNOLOGIES•INC, http://www.microfab.com/images/pdfs/v.4/jetlab2_mf5.pdf

[11] "Capillary Action – Liquid, Water, Force, and Surface – JRank Articles". Science.jrank.org. Retrieved 2013-06-18.

[12] Manos Anyfantakis,Zheng Geng, Modulation of the Coffee-Ring Effect in Particle/Surfactant Mixtures:the Importance of Particle−Interface Interactions, DOI: 10.1021/acs.langmuir.5b00453 Langmuir 2015, 31, 4113−4120

[13] Sivananda S. Jada, Study of Tetraethyl Orthosilicate Hydrolysis by in Situ Generation of Water, DOI: 10.1111/j.1151-2916.1987.tb05640.x

APPENDIX A

TOP VIEW SEM IMAGES OF SAMPLES PRINTED USING METHANOL,
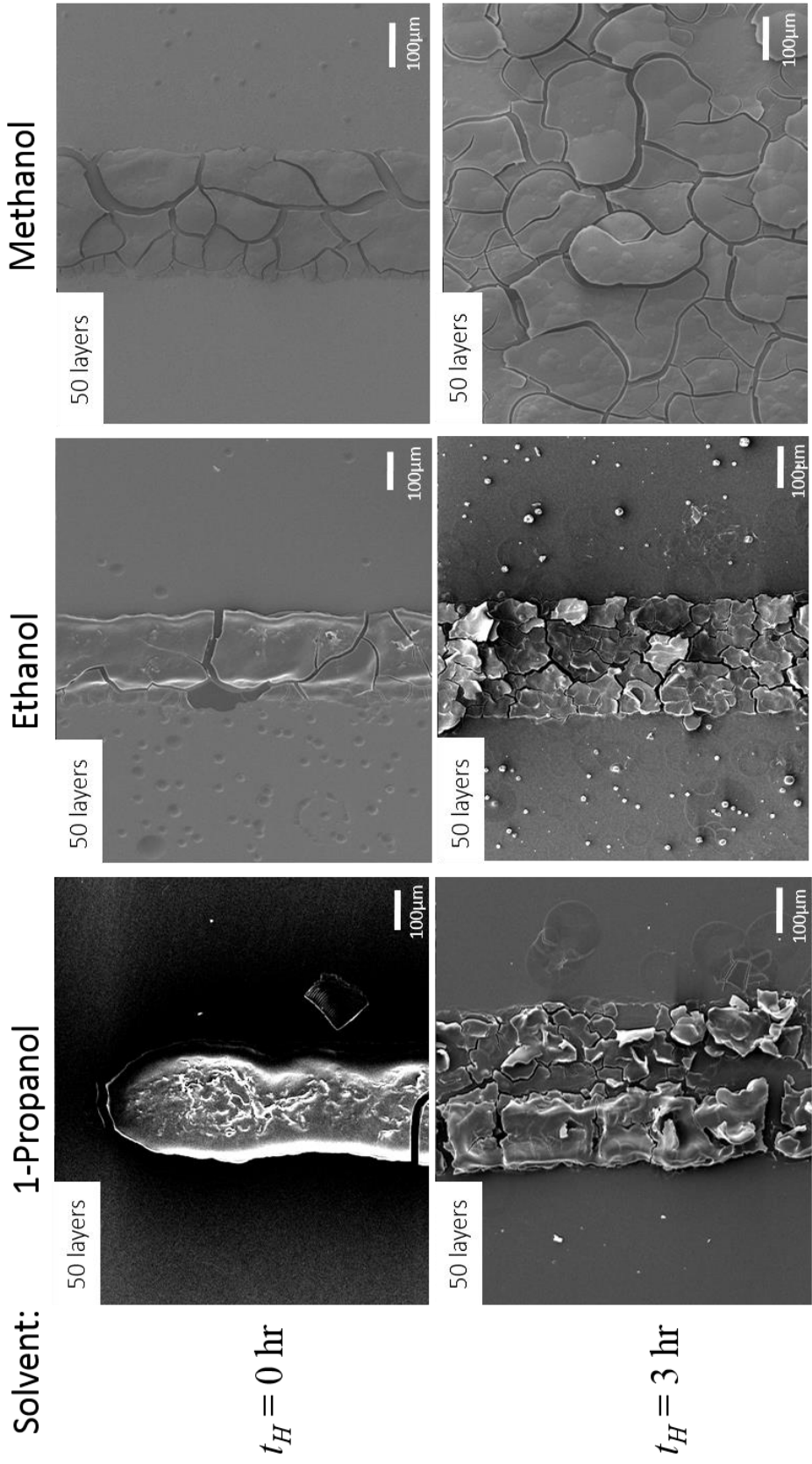
ETHANOL AND 1-PROPANOL AT DIFFERENT TEMPERATURES.

|	50 ℃	75 ℃	100 ℃	125 ℃
Methanol 64 ℃				
Ethanol 78 ℃				
1-Propanol 98 ℃				
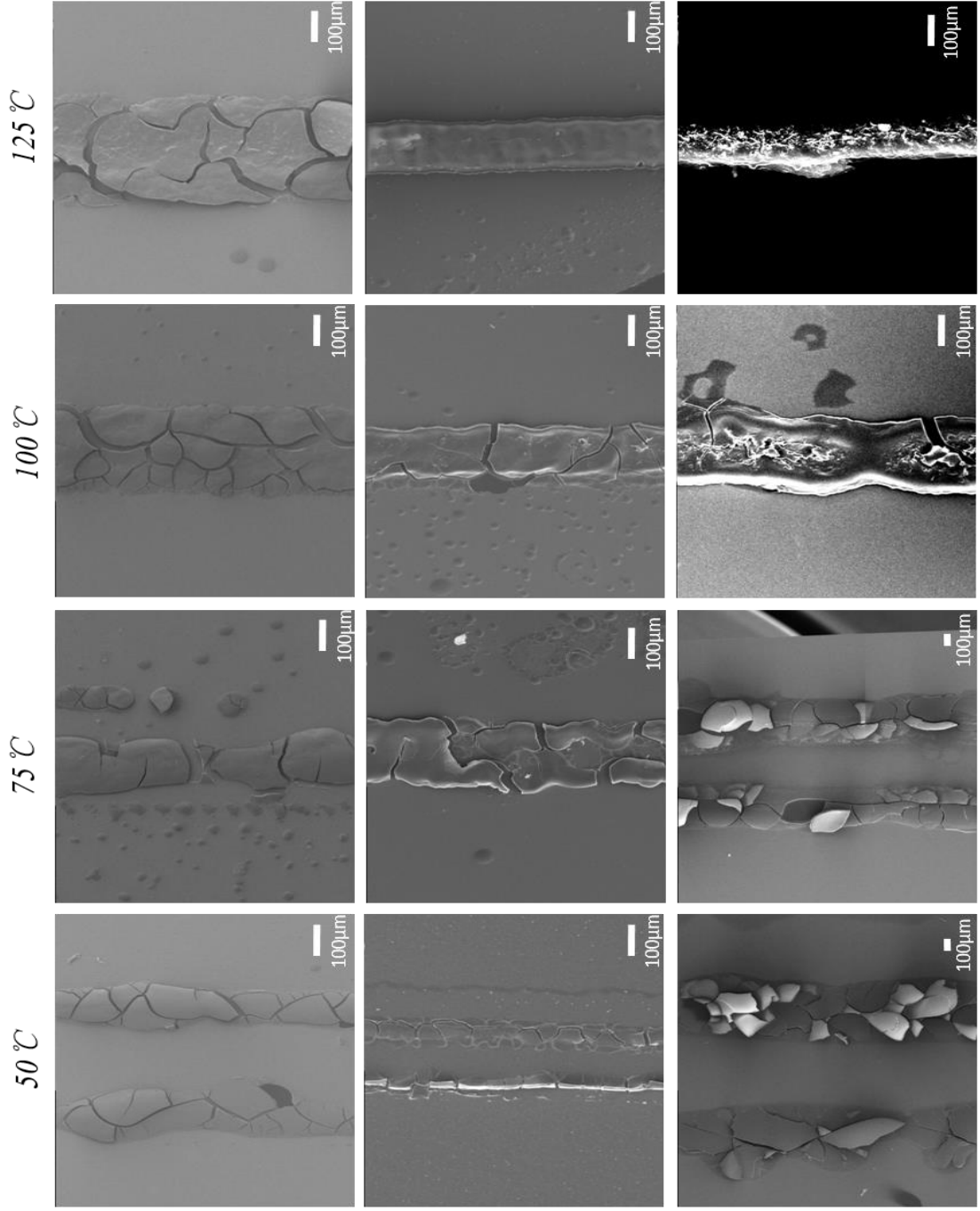
APPENDIX B

MORPHOLOGY OF PRINTED LINE USING REACTIVE AND FULLY

HYDROLYZED INKS DILUTED BY METHANOL, ETHANOL AND 1-PROPANOL.

Solvent: 1-Propanol   Ethanol   Methanol

$t_H = 0$ hr

$t_H = 3$ hr

50 layers (all panels)   100μm (scale bars)

37

APPENDIX C

TOP VIEW AND CROSS SECTION VIEW OF PRINTED LINES USING ETHANOL

DILUTED REACTIVE INK AT 125℃. SOLID LAYER BY LAYER STRUCTURES

ARE OBSERVED IN HIGH MAGNIFICATION IMAGES.

50 layers

100μm

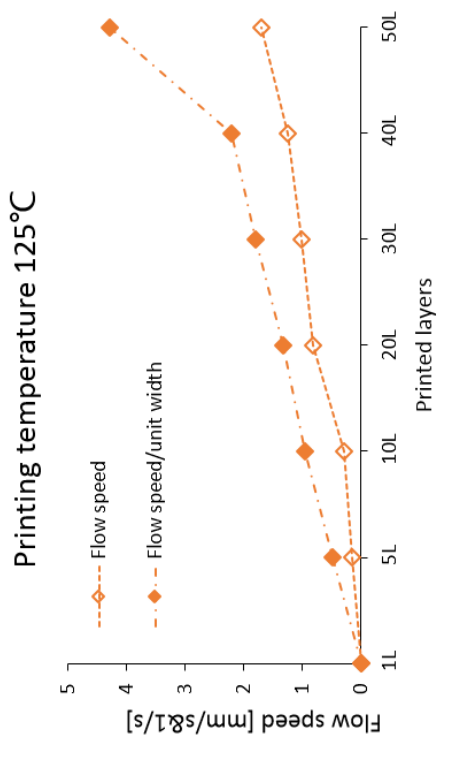50 layers

1μm
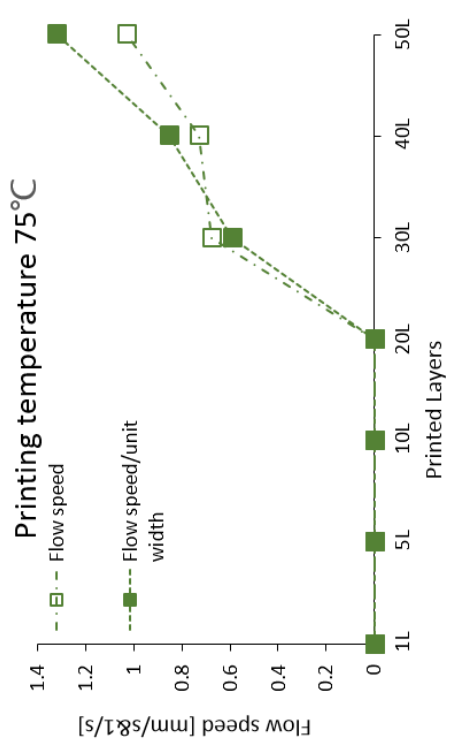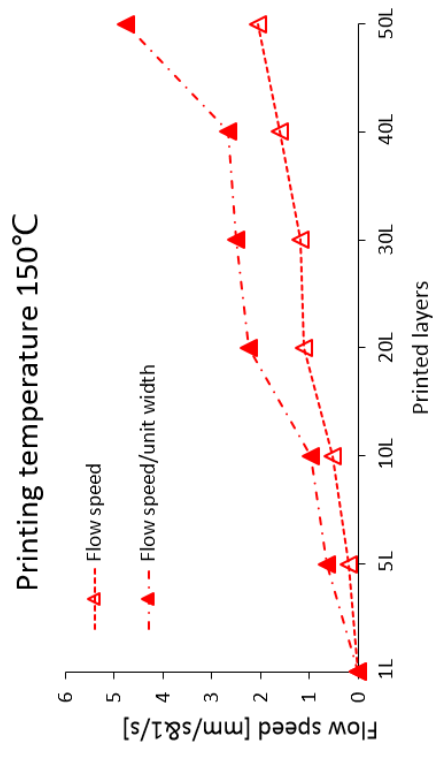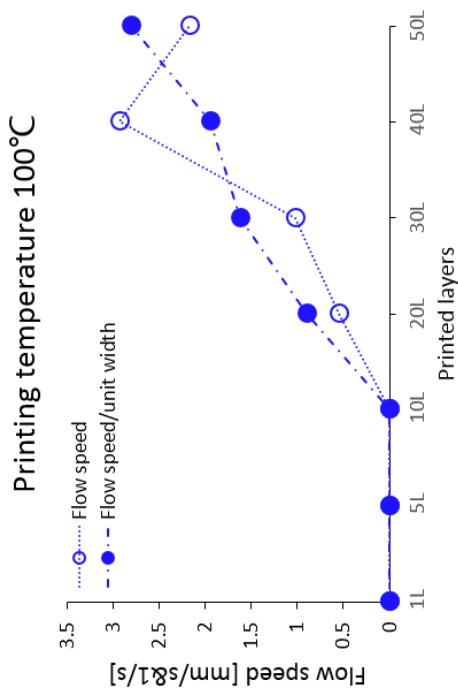

50 layers

100μm

50 layers

10μm

39
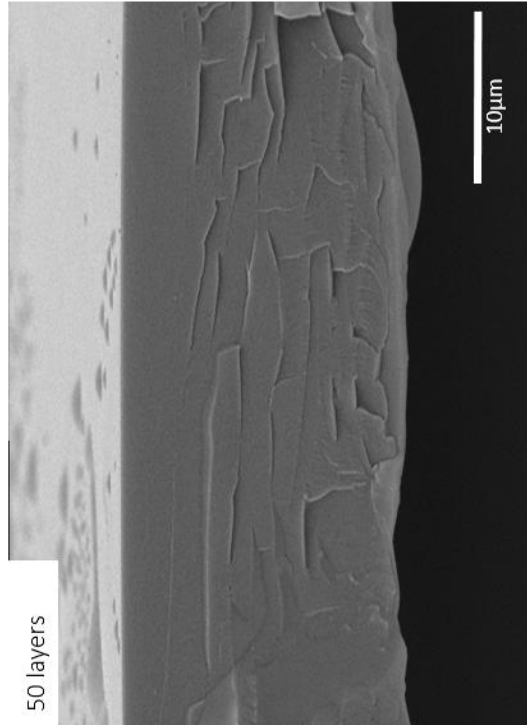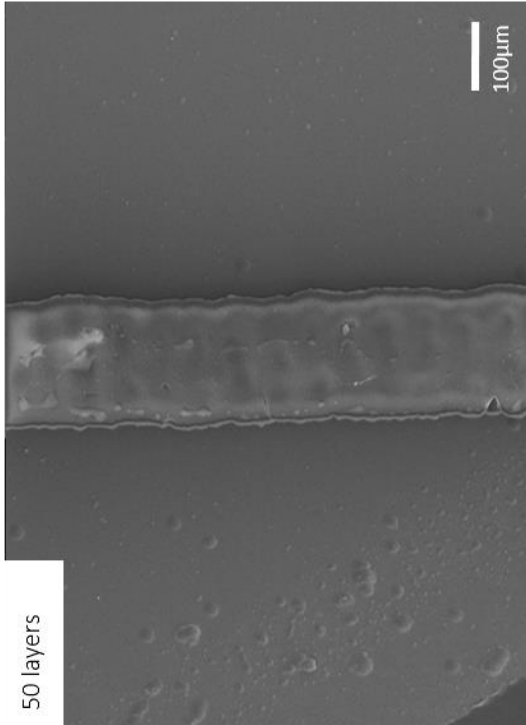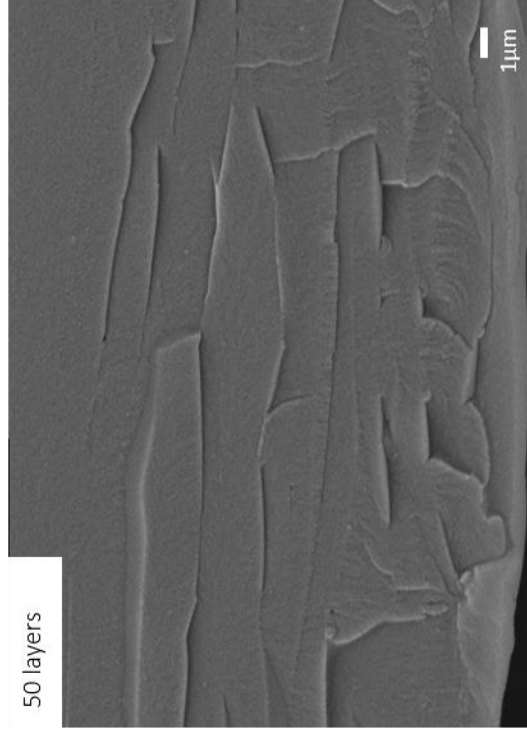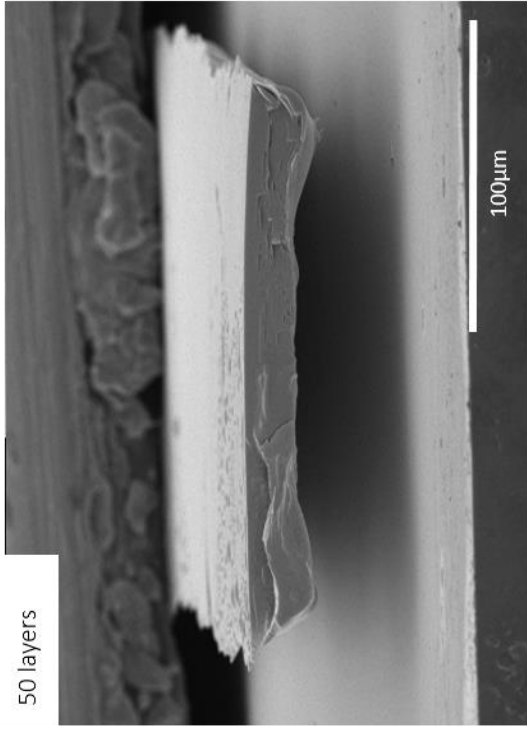
APPENDIX D

TOP VIEW OF PRINTED LINES USING ETHANOL DILUTED FULLY

HYDROLYZED INK AT 125℃, FRACTURE MORPHOLOGY AND ROUGH

SURFACE FORM IDEAL CONDITION FOR CAPILLARY ACTION.

50 layers

10μm

50 layers

100μm

41
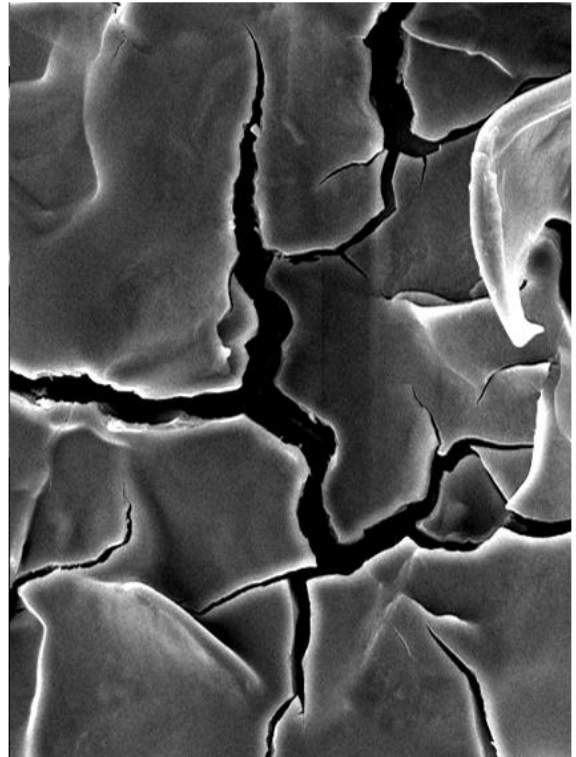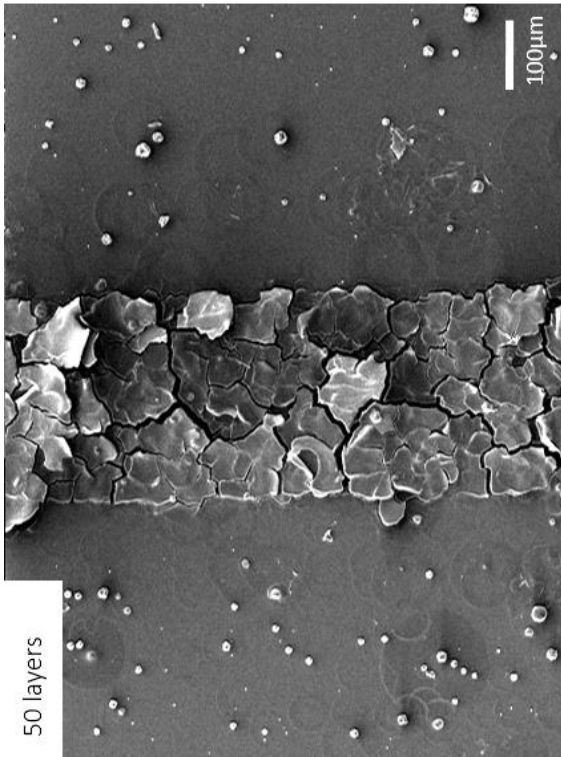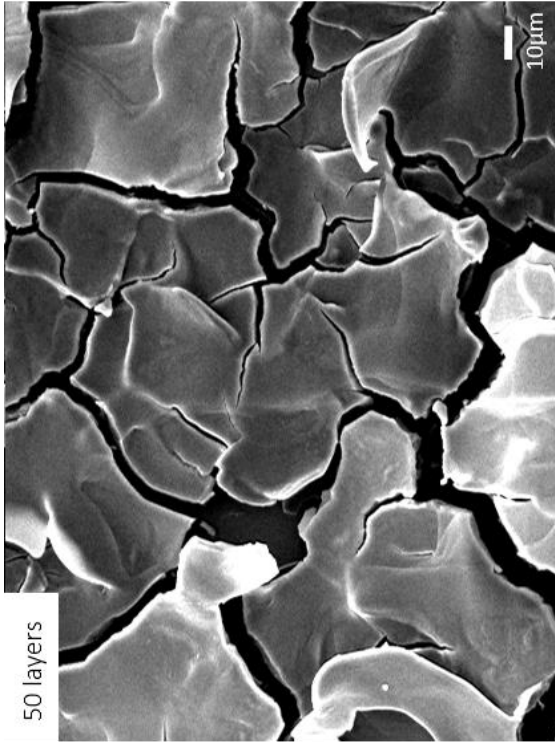
APPENDIX E

FLOW SPEED AND FLOW SPEED PER UNIT WIDTH *VS.* PRINTED LAYERS AT

75, 100, 125, 150℃

APPENDIX F

COMPARISON OF FLOW SPEED PER UNIT WIDTH *VS.* PRINTED LAYERS AT

DIFFERENT SUBSTRATE TEMPERATURES